Development of an educational setup for practical applications of strain gauges

Laurin Rossmeier, Franz-Josef Falkner (supervisor)

***Abstract*—This master thesis presents the development of an educational setup for practical applications of strain gauges, designed to bridge the gap between theoretical concepts and hands-on experience in engineering measurements. The setup addresses static measurements of strain, torsion, bending, and normal forces using various bridge configurations including quarter-bridge, half-bridge, and full-bridge topologies.A complete measurement system was developed, featuring a custom-designed measurement amplifier with switchable bridge completion, shunt calibration, and analog filtering. The amplifier's performance was benchmarked against industry-standard equipment, showing comparable noise characteristics. A microcontroller-based data acquisition and processing system was implemented, providing real-time measurement display and data output. The mechanical design includes a series of probes for different loading scenarios, including a custom S-shaped load cell, a torsion bar, a bending beam, and a tension probe. Each probe was designed and optimized using analytical calculations or finite element analysis. Extensive testing and evaluation were conducted to characterize the system's performance, including noise measurements, non-linearity assessments, and hysteresis calculations for each probe. The results highlight both the capabilities and limitations of the developed setup, providing valuable insights for future improvements.**

***Index Terms*—strain gauge, force measurement, measurement bridge, instrumentation amplifier, engineering education.**

I. Introduction

STRAIN gauges are fundamental sensors widely used in engineering applications to measure deformation, stress, and force. Despite their prevalence, many engineering students lack practical experience with strain gauge measurement techniques and their limitations. This thesis addresses this gap by developing an educational setup that bridges theoretical knowledge and practical application of strain gauge measurements.

The educational setup focuses on static measurements of strain, torsion, bending, and normal forces using various bridge configurations, including quarter-bridge, half-bridge, and full-bridge topologies. These configurations are essential for understanding the operational principles of strain gauges, which rely on the change in electrical resistance of a conductor when subjected to mechanical stress. The Wheatstone bridge circuit, a fundamental component in strain gauge measurements, is employed to convert resistance changes into measurable voltage outputs. Different bridge configurations offer varying levels of sensitivity, temperature compensation, and complexity.

Understanding and addressing errors is crucial for accurate strain gauge measurements. Systematic errors, such as those from temperature changes, gauge factor variations, and transverse sensitivity are explained and mitigated through calibration and compensation techniques. Random errors, including those caused by electrical noise and mechanical vibrations are similarly analyzed. Mitigation strategies for these errors involve design choices and filtering methods to enhance measurement precision.

By providing a unified, portable experimental setup, this project enhances engineering education in strain measurement techniques. It allows students to gain practical insights into strain gauge selection, installation, bridge configurations, signal amplification, and data analysis. The open design also permits future expansions to explore more topics in experimental stress analysis.

II. Methods

This section describes the experimental setup and methodologies used to design strain gauge applications. It details the mechanical and electrical design considerations, focusing on the design and implementation of the measurement amplifier system and the mechanical dimensioning on the example of the torsion experiment.

Laboratory Setup

The measurement setup is designed to provide a solid and flexible educational platform for different strain gauge applications. The developed system's block diagram is shown in Figure 1. It shows the four primary experiment probes for tension, bending, torsion, and force which can each be connected to the same connector one at a time.

A 4-way selector switch then enables the selection of the desired bridge completion for the 3-wire quarter bridge, quarter bridge, half bridge and full bridge configurations.

The Bridge Completion resistors are equipped with coarse and fine shunt calibration potentiometers to adjust the zero point. Following up with the measurement amplifier that amplifies the signal to be suitable for the data acquisition system. The acquired measurement data is then displayed and provided for external processing via UART.

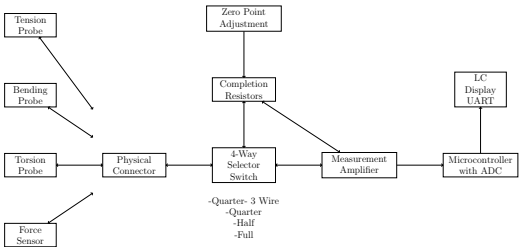

Fig. 1: Block diagram of the measurement setup.

Measurement Circuit

Figure 2 illustrates the electrical implementation of the design developed in figure 1. The challenge hereby is not to introduce imbalances due to contact and additional wire resistances. The developed scheme is designed to keep the contact resistances as symmetrical as possible.

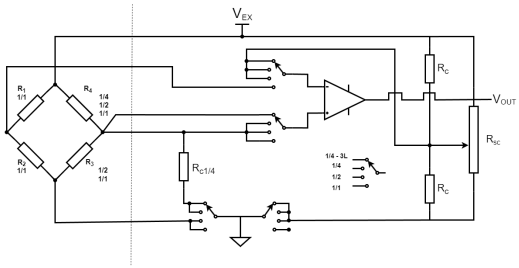

Fig. 2: Scheme of the measurement circuit.

The vertical dashed line represents the connector interface. On the left side of the dashed line, the different measurement topologies are connected. If for example a quarter bridge configuration is needed, only strain gauge R_4 is connected to the required connector terminals. Everything to the right of the dashed line always stays the same, apart from the selected position of the switches, which are mechanically coupled. This means, that the arrow in each switch always point at the same poles like shown in this case for the 3 wire quarter bridge configuration. The shunt calibration potentiometer R_{SC} is connected parallel to the quarter- and half bridge completion resistors R_C this allows bridge balancing in quarter and half bridge mode. The shunt calibration of the full bridge has to be performed on the measurement location.

In order to verify, that the measurement circuit developed in figure 2 functions as desired a SPICE simulation is performed. The program LTspice is used to simulate the instrumentation amplifier combined with the switchable completion resistors.

The simulation setup for the full bridge can be seen in figure 3. The manual switch is simulated using a

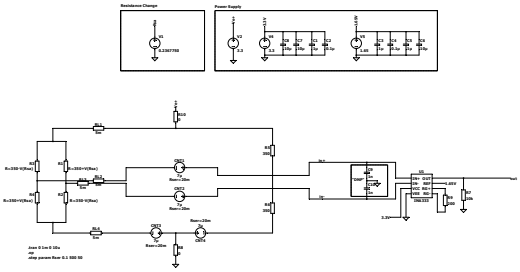

Fig. 3: LTspice schematic of the full bridge measurement amplifier.

voltage source with a defined series resistance. The series resistance acts as the contact resistance and the voltage simulates thermal voltages of the contacts.

The Seebeck effect creates a thermal voltage when there is a temperature difference across different metals. This can be calculated using the Seebeck coefficient S for each material.

For the proposed rotary switch, gold-plated contacts are used to transfer current to and from a silver-plated rotor. The worst-case scenario is modeled with a $1\,\mathrm{K}$ temperature difference between input and output contacts, split into two $0.5\,\mathrm{K}$ transitions.

After modeling the material transitions from the copper wire through solder joints and the switch a worst case thermal voltage of $7\,\mu\mathrm{V}$ is determined. This voltage along with a contact resistance of $20\,\mathrm{m}\Omega$ derived from datasheets is used in the simulation to model the worst-case scenario for the rotary switch.

Like for the full bridge seen in figure 3 the circuit was also adapted for the remaining three topologies. With this simulation it can be determined how big of an impact the contact effects have on the measurements in the worst case.

The Printed Circuit Board (PCB) organizes all the necessary components of the previously determined design onto a generously sized board. The layout is optimized to minimize signal path lengths while positioning amplifier components roughly according to the printed schematic. Bridge completion resistors are located on the bottom of the pcb, connected to solder terminals for switch and potentiometer wiring. The STM Nucleo microcontroller is mounted using pin sockets for easy removal or replacement. Jumpers allow mapping of the measurement signal to various analog input pins of the microcontroller. Connector P16 serves as the interface for the LCD screen. LEDs are placed on the marked switch locations to indicate the active signal paths.

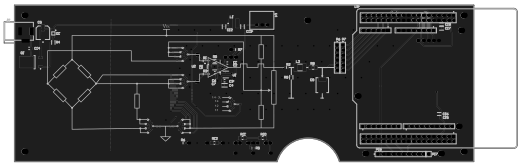

Fig. 4: PCB of the measurement amplifier.

Mechanical Design

Each experiment features a probe that utilizes a different application, shape, or topology of one or more strain gauges. To create a valuable learning environment, each probe must be designed to achieve consistent strain readings on the measurement amplifier. The probes are strained by applying weights to exert force. Since the setup needs to be portable, the amount of weight is limited to about $5\,\mathrm{kg}$. The designed loading setup, as seen in Figure 5, is uniform across all experiments and consists of several discs with different masses that can be stacked.

Probe Design: To demonstrate the process of designing the experiments the process for the torsion experiment are elaborated. First, the general shape of the experiment is defined in figure 7. the torsion probe features a circular cross-section and is fixed on one side. A torque arm is attached on the other end onto which the load is applied. At the junction of the torque arm and torsion bar, the bar is radially supported to prevent any bending.

The torsion bar is equipped with a half-bridge XY [1] strain gauge, seen in figure 6, where the

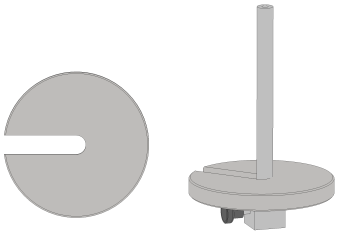

Fig. 5: Weights and attachment rod.

Fig. 6: Used HBM XY strain gauge [1].

measuring grid axes are oriented at $\pm 45^\circ$ to the axis of symmetry. This is specifically designed for torque measurement application, as the principal strain direction is aligned with the planes of maximum normal strains for cylindrical shafts.

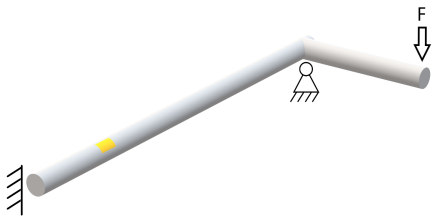

Fig. 7: Torsion bar.

For dimensioning the cylindrical torsion probe using a half-bridge strain gauge configuration, the following formulas are used [2]:

When using a half bridge, the mesured strain value ε_a is given by:

$$\varepsilon_a = 2\varepsilon \tag{1}$$

The maximum shear stress τ_{max} at the surface of the cylinder then is calculated using the shear modulus G of the used material:

$$\tau_{\text{max}} = \varepsilon_a G \tag{2}$$

The torsional moment M_t is calculated as:

$$M_t = \varepsilon_a G W_p \tag{3}$$

For a cylindrical shaft with a diameter d, the polar section modulus W_p is:

$$W_p = \frac{\pi d^3}{16} \approx 0,2 d^3 \tag{4}$$

Knowing the applied force F_t and the length of the torque arm l_t the torque M_t applied to the torsion bar is given by:

$$M_t = F_t l_t \tag{5}$$

Considering these equations, material parameters and manufacturabilty constrains following specifications were defined for reaching a required target strain of ε = 0.001 66.

- Material: Aluminum
- Diameter, d: 12 mm
- Length, L: 220 mm
- Torque Arm Length, l_t: 150 mm
- Maximum Applied Load, F_t: 50 N

The CAD model in Figure 8 details the mechanical construction, highlighting the radial support provided to prevent bending and ensure accurate torsional measurements. The design allows for precise application of torque, by placing different configurations of weight discs on the loading arm.

While similar approaches can be taken to design the bending and tension probe, the design of the load cell requires a different approach. The proposed design for the load cell seen in figure 9 uses a widely adopted configuration that incorporates two holes in

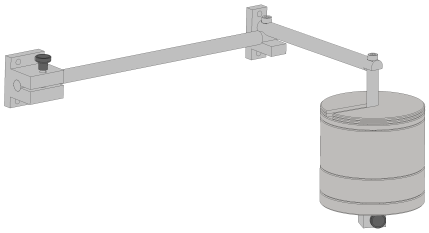

Fig. 8: Mechanical construction of the torsion experiment.

a beam, creating four symmetrical deformation zones for tension and compression. L-shaped mounting arms at each end ensure perfect axial loading, which is required for accurate measurements. By utilizing four strain gauges in a full-bridge configuration, the design achieves high sensitivity, temperature stability, and low noise.

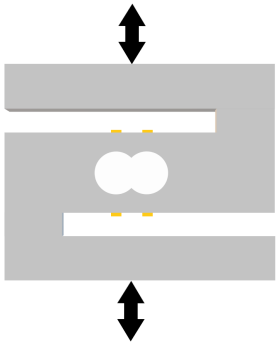

Fig. 9: Draft of the load cell.

Analytical calculation of strain in the deformation areas of this geometry is exceedingly complex. To address this challenge, numerical Finite Element Method analysis using ANSYS is employed.

The design process therefore begins with creating an initial geometry, which is parameterized to facilitate optimization. After establishing the geometry, materials are assigned to ensure that the model's properties align with its intended application. A mesh is then generated, with particular refinement around the areas where strain gauges will be placed, to accurately capture strain distribution in these critical zones.

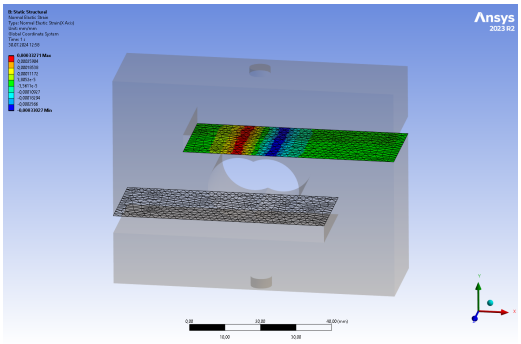

Fig. 10: Normal elastic strain in the x-direction.

During simulation setup, the lower mount of the load cell is fixed to accurately simulate boundary conditions. A force of 50 N is applied to the top mount to represent the operational loading condition. The normal elastic strain in the x-direction is plotted in figure 10, providing essential visualization for assessing strain distribution and identifying areas of maximum strain.

The geometry optimized to achieve the desired strain in ANSYS is then reproduced in Autodesk Inventor with considerations for manufacturability and assembly. The L shaped mounting brackets are created as separate pieces and attached to the main body using bolts. This is necessary, since it would be hard to apply the strain gauges otherwise.

1) Application of Strain Gauges: The application of strain gauges requires high precision and a steady hand. First, the material must be prepared for gluing the strain gauge. The surface should be smooth, with a random sanding pattern. The location of the strain gauge then has to be marked as seen in image 11a,

keeping score marks as minimal as possible. Image 12b shows the bending beam application where a laser engraver was used to precisely project a minimal invasive gauge alignment pattern into the surface.

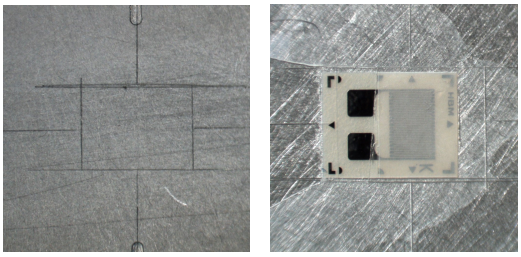

(a) (b)

Fig. 11: a) Markings for strain gauge placement and b) glued on strain gauge.

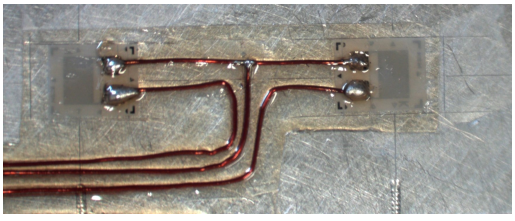

(a)

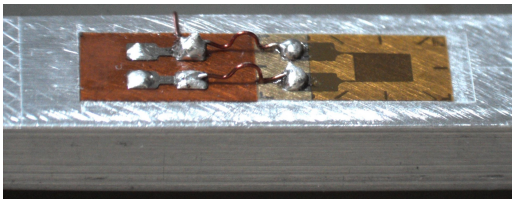

(b)

Fig. 12: Solder connections of the a) load cell b) bending beam.

After degreasing the surface, the strain gauge is positioned and glued. Even pressure is applied with non-stick Teflon until the adhesive dries. Adhesive tape helps with precise positioning and prevents adhesive from covering the solder pads.

For connecting the strain gauge to a measurement circuit, wires are soldered to the delicate connection terminals. A jumper wire is used to create a more robust connection terminal away from the strain gauge. The load cell strain gauges seen in figure 12a are connected in a full bridge topology with red wires leading to a solidly mounted terminal. For the bending probe, a separate solder pad terminal seen in figure 12b is glued next to the strain gauge, with small jumpers connecting one side and the cable on the other. This setup protects the strain gauge by breaking between the solder points if excessive force is applied.

III. Results

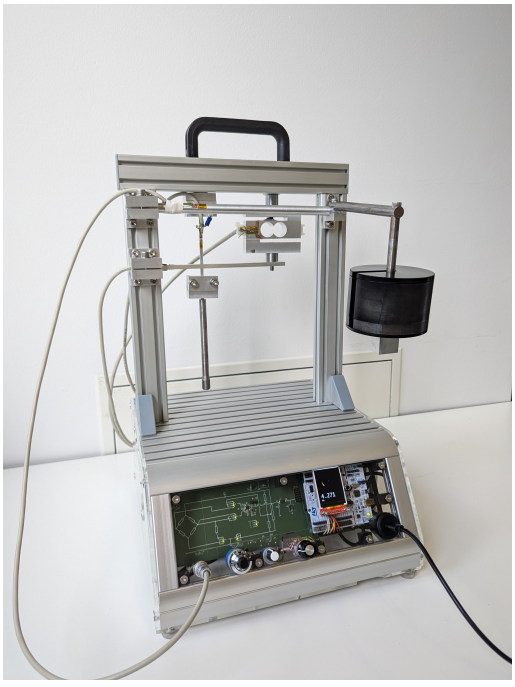

Fig. 13: Torsion probe experiment setup.

Figure 13 shows a picture of the developed lab setup with a torsion experiment. The design is realized using aluminium extrusions and acrylic panels.

It is portable and allows for independent use of the different load configurations. The upper section of the setup is designed to house the mechanical probes. The lower section accommodates the electronics and user interface. To maximize space utilization, a drawer is incorporated into the rear section of the lower compartment, providing storage for additional lab equipment. The user interface can be seen with the three knobs for bridge selection and coarse / fine shunt calibration. The screen shows the measured value and unit as well as an animation for each probe that is scaled accordingly for a more intuitive experience. display mode toggle button is positioned on the screen's right side.

A. Performance Measurements

1) Electrical: Based on the electrical simulations mentioned in section II the switch introduces a maximum error of $35.76\,\mu\mathrm{V}$ into the measurement signal. This relates to about $1\,‰$ of the full measurement scale, which is pretty much negligible.

These simulation results were necessary to validate the electrical design for manufacturing. To assess the performance of the finished electronics, noise measurements were performed. To measure the noise, a load cell is left unloaded and shielded in a constant environment from major mechanical vibrations and temperature fluctuations for all measurements. The output signal resulting from a $3.3\,\mathrm{V}$ excitation is then captured for $12\,\mathrm{s}$ using different data acquisition hardware.

The comparison of the power spectral density seen in figure 14 of the NI 9237 against the 2934 provides the most reliable comparison of the amplifier stages, since the ADC of the two measurement cards are very similar. These measurements reveal that the NI 9237 outperforms the developed amplifier above $1\,\mathrm{Hz}$ in terms of noise performance by approximately $10\,\mathrm{dB\,Hz^{-1}}$. The implications of this finding are concluded in IV.

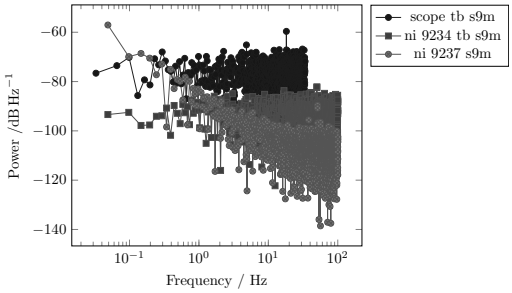

Fig. 14: Power spectral density of different measurement devices.

TABLE I: RMS Noise Measurements for different Probes.

DAQ	Amplifier	Sensor	RMS Noise / mV
Scope	Testboard	s9m	1,085
Scope	Measurementboard	lc	0,918
Scope	Measurementboard	toque	0,647
Scope	Measurementboard	bending	1,946
Scope	Measurementboard	tension	5,269
Scope	Measurementboard	tension 3 Wire	5,249

Table I shows the RMS noise of each experiment probe. It can be seen, that the self developed load cell has similar behavior as the HBM S9M reference device. The torsion probe has the lowest noise reading, even lower than the load cell. Despite also having a half bridge topology, the bending probe has far worse noise behavior than the torsion probe. The tension probe has the highest noise susceptibility.

2) Mechanical: Non-linearity and hysteresis are important characteristics in mechanical measurement systems. These parameters are determined by applying forces over the full range of the sensor in both ascending and descending order. The maximum deviation of the measured output from a straight line is the non-linearity. The hysteresis is the maximum difference between the same ascending and descending measurement.

Table II shows the measurement results for the torsion probe

TABLE II: Non-linearity (NL) and hysteresis measurements for the torsion probe.

Force In N	Asc.	Desc.	Non-Linearity Base line	Non-Linearity Asc. In $\%FS$	Non-Linearity Dsc. In $\%FS$	Hysteresis in $\%FS$
0,00	2048	2053	2048,0	0,00	0,59	0,59
1,25	2033	2027	2027,1	0,71	0,01	0,71
2,50	2014	2006	2006,1	**0,94**	0,01	0,95
5,00	1970	1967	1964,2	0,69	0,33	0,36
10,00	1884	1876	1880,4	0,43	0,52	0,95
20,00	1710	1700	1712,8	0,33	**1,52**	**1,19**
30,00	1543	1537	1545,2	0,26	0,97	0,71
40,00	1377	1375	1377,6	0,07	0,31	0,24
50,00	1210	1210	1210,0	0,00	0,00	0,00

The maximum values are highlighted in bold. While these results are not great on compared to standard precision equipment, other probes performed significantly worse. The bending probe achieved a non-linearity of $2.44\,\%$ under reduced loading conditions, the load cell $8.41\,\%$ and the tension probe renders almost useless at $44.08\,\%$. Reasoning for this performance is concluded in section IV.

IV. Conclusion

The project resulted in the development of a comprehensive educational setup for strain gauge applications. This setup includes a solid, portable platform housing various mechanical probes such as a load cell, torsion probe, bending probe, and tension probe, each designed to demonstrate different strain measurement scenarios. A custom measurement amplifier with switchable bridge configurations was created, incorporating features like shunt calibration and digital filtering. The system integrates a microcontroller for data processing and a user interface with an LCD display for real-time measurement visualization. While the electrical components performed well, the mechanical probes lack in accuracy and linearity, indicating areas for future refinement and improvement.

A. Electrical Performance

The developed measurement amplifier has a noise floor of roughly $-90\,\mathrm{dB\,Hz^{-1}}$, which is excellent performance considering the open and widespread PCB design in a unshielded case using acrylic panels is not ideal for noise susceptibility.

B. Mechanical Probes

Based on the findings from previous sections, it is evident that the mechanical probes in their current state do not provide an optimal learning environment. The significant impact of proper loading and the low sensitivity of some probes render them impractical for laboratory experiments.

A comprehensive redesign of all probes is necessary to create an effective learning environment. This redesign should use the tension probe as a baseline for calculations. Furthermore, the attachment points for both the probe and weight should be redesigned, incorporating ball joints or similar mechanisms to ensure consistent and accurate measurements. Enhancements in mechanical precision through CNC milling and improved bridge balancing could elevate the load cell's performance.

References

[1] Hottinger Baldwin Messtechnik GmbH, *HBM-A Serie*, Hottinger Baldwin Messtechnik GmbH, 2024. [Online]. Available: https://www.hbm.com/fileadmin/mediapool/hbmdoc/technical/B0539

[2] K. Hoffmann, *An Introduction to Measurements using Strain Gages*. Darmstadt: Hottinger Baldwin Messtechnik GmbH, 1989.

Laurin Rossmeier is a Master student of the Mechatronics program at MCI Innsbruck, majoring in electrical engineering. His interests and technical knowledge span a wide range of technical fields from microcontroller programming, electronics design, mechanical design and manufacturing all the way to woodworking.